

Characterization and Comparison of 3D Printed Substrate with Varying Infill Density for Antenna Design Applications

Kush Singla¹, Balwinder S. Dhaliwal² and Garima Saini³

^{1,2,3} National Institute of Technical Teachers Training & Research, Chandigarh, 160109, India

Abstract:

Characterization and comparison of 3D printed materials based on acrylonitrile butadiene styrene (ABS) filament for antenna design are presented in this paper. The standard ring resonator method has been used to obtain the dielectric properties of the material, where a ring is excited from two ports and its resonance characteristics are used to calculate dielectric characteristics. The effect of different infill densities of the printed substrate on dielectric constant and loss tangent has been thoroughly analyzed. The results obtained are helpful for the antenna design applications for desired frequency of 2.45 GHz, using variation in the dielectric constant and dielectric loss.

Keywords

3D-printed antenna, acrylonitrile butadiene styrene (ABS), dielectric properties, infill density, infill pattern, loss tangent, additive manufacturing.

1. Introduction

To get smart engineering solutions 3D printing is used for rapid prototyping for major industrial applications. The low cost and high throughput sector with a less resource requirement for massive production and customization are evolving due to 3D printing. Fast prototyping, less wastage of material, design flexibility and low-cost development are some of the advantages offered by 3D printing in the field of RF applications. Fused deposition modeling (FDM) is the most used approach among all the different 3D printing techniques. It has also been used for printing polymeric materials for RF and microwave applications. FDM is an extrusion-based method in which the object is formed layer by layer, a plastic filament is melted and placed on the 3D printer platform. During extrusion, a 2D layer of material is placed accurately by the extruder [1][2]. Hence, a 3D structure is formed by overlapping 2D layers of material. Commercial printers deposit layers with height ranging from 50 μm to 300 μm and the technology is easy to use and cost-effective.

FDM fabrication process using commercial thermoplastic called Acrylonitrile Butadiene Styrene (ABS) is presented in this paper. Infill density is one of the important parameters in 3D printing [3]. In this paper, two infill densities have been considered i.e. 40% and 100%. For this paper, the lowest and the highest possible infill density is considered, and their results are compared. The idea behind choosing only these two infill densities was that infill density below 40% leads to a lot of air pockets in the design which is not good for RF characteristics. Rectilinear infill pattern is chosen for this paper [4] tells it's the best pattern for RF characterization. Samples with varying infill densities are printed for evaluating the dielectric properties of the printed substrates. High-frequency structure simulator (HFSS) software has been used for designing the ring resonator structure and to obtain the dielectric properties of the material. Moreover, a comparison of the antenna substrate with different infill densities is also presented.

International Conference on Emerging Technologies: AI, IoT, and CPS for Science & Technology Applications, September 06–07, 2021, NITTTR Chandigarh, India

EMAIL: ksingla02@gmail.com; bsdhaliwal@ymail.com; garima@nitttrchd.ac.in

ORCID: 0000-0001-6558-9192; 0000-0001-5092-017x; 0000-0001-6525-5192

©2021 Copyright for this paper by its authors.

Use permitted under Creative Commons License Attribution 4.0 International (CC BY 4.0).



CEUR Workshop Proceedings (CEUR-WS.org)

2. Characterization of dielectric material

To calculate the dielectric properties of the 3D printed substrate at the desired resonance frequency of 2.45GHz, a standard ring resonator approach has been used[5][6]. Figure 1 displays dimensional details of the structure:

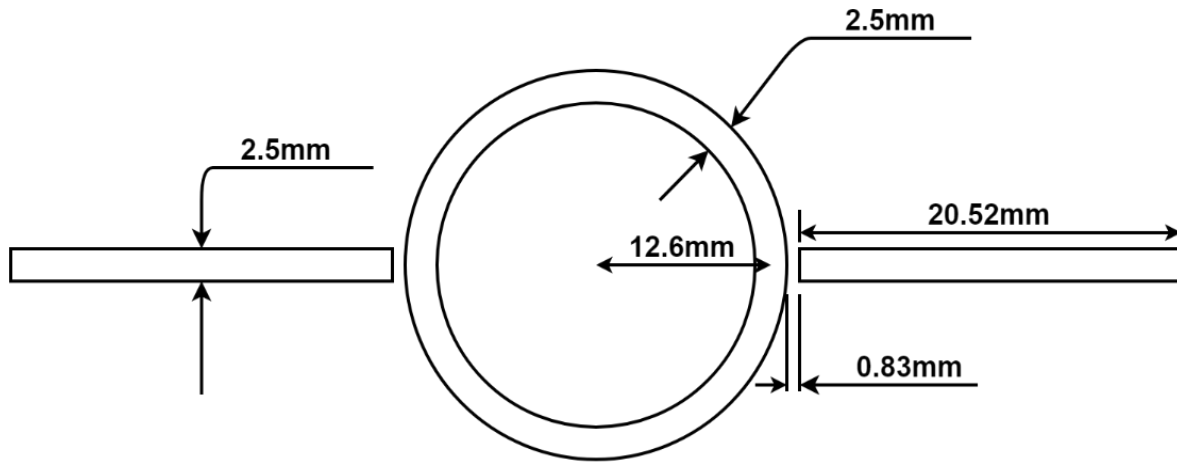


Figure 1: Dimensions of the microstrip ring resonator.

Figure 1 displays structure of the ring resonator, dimensions of microstrip feeding lines, the ring gap, and the average radius, r_m .

Figure 2 shows the fabricated ring resonator structures having SMA connectors soldered at the edges of the feed lines. Figure 2(a) shows the 40 % infill density & rectilinear infill pattern substrate and Figure 2(b) shows the 100 % infill density & rectilinear infill pattern substrate.

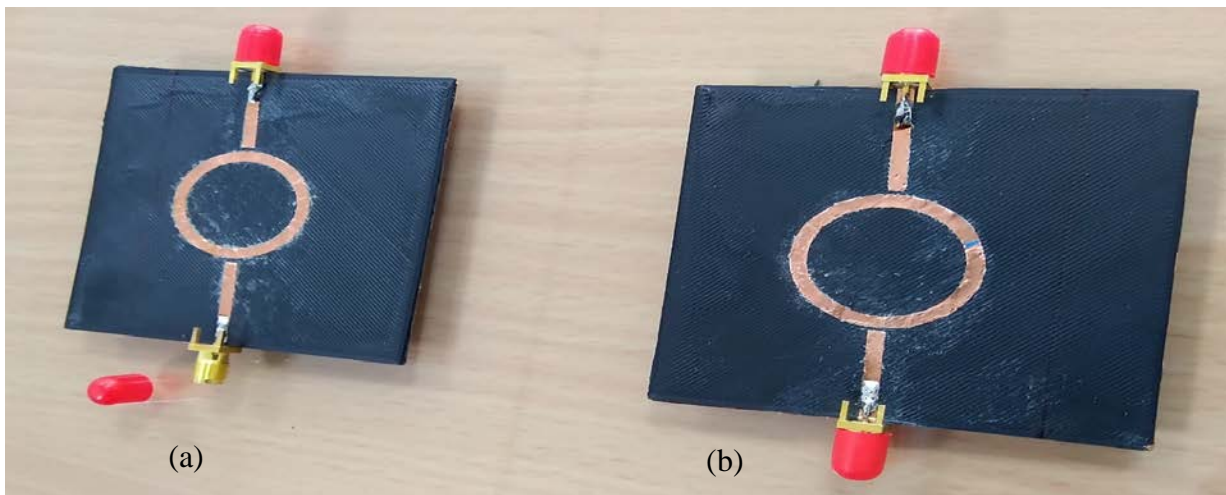
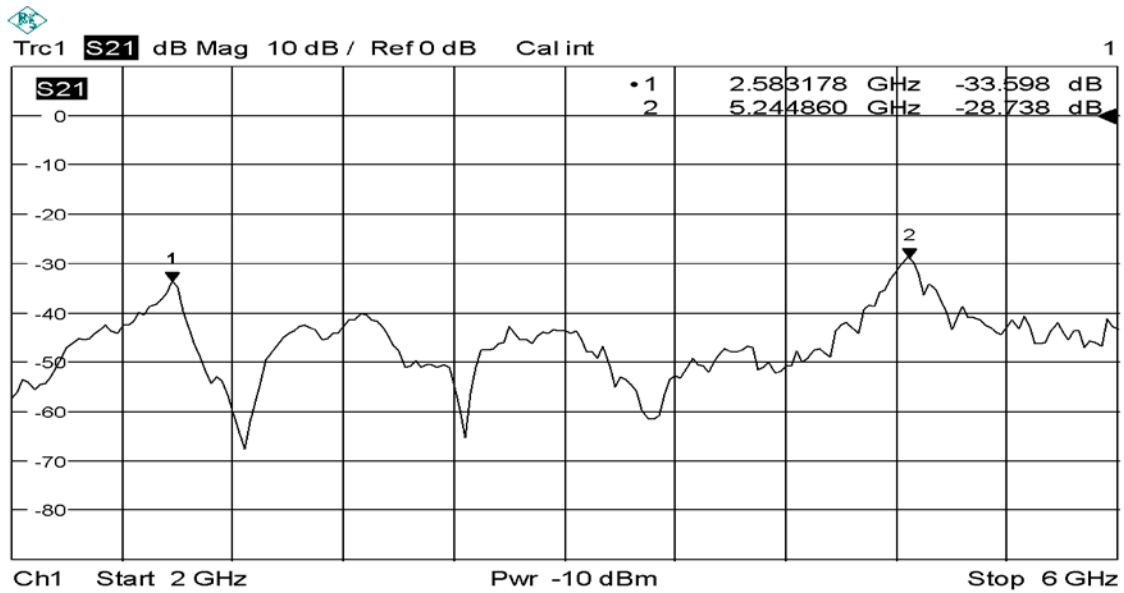


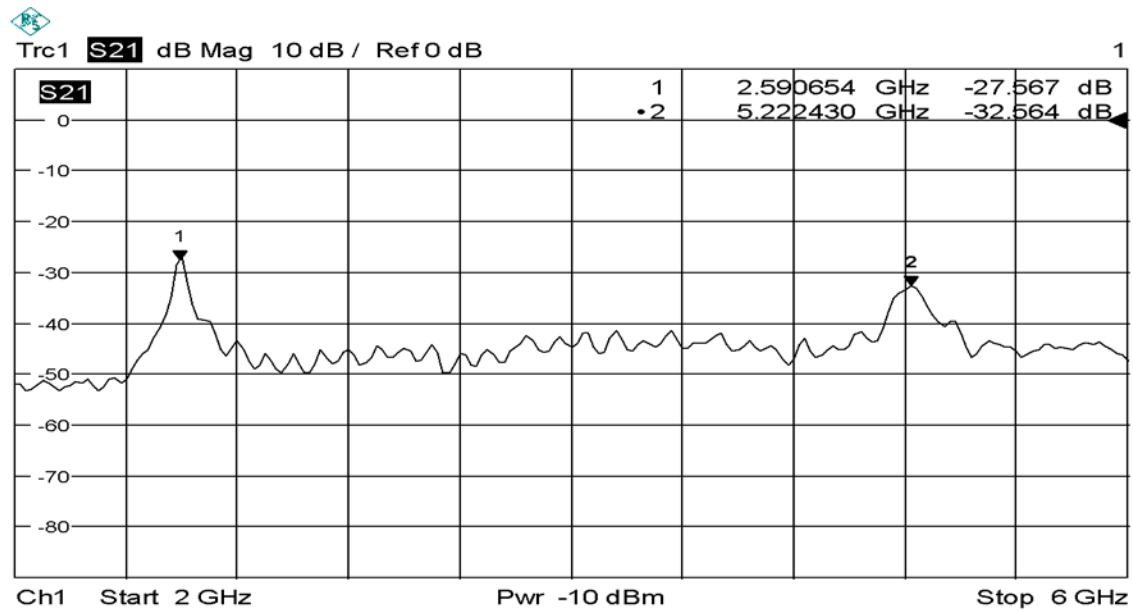
Figure 2: Ring resonator structures on substrates with (a) 40% Infill density (b) 100% Infill density.

Periodic frequency resonances are generated by insertion loss (S_{21}) produced by the ring resonator. Using this approach, with the given radius of 12.6mm ring resonator, dielectric constant (ϵ_r) can be obtained from the location of resonant peaks of the ring resonator. Quality factor (Q) of resonant frequency peaks

is used to obtain the value of dielectric loss ($\tan\delta$). Figure 3 shows the plot of S_{21} as a function of frequency for both the substrates. Figure 3 values are obtained using a vector network analyzer.



(a) The measured S_{21} for 40% infill density and rectilinear infill pattern on vector network analyzer (VNA).



(b) The measured S_{21} for 100% infill density and rectilinear infill pattern on vector network analyzer (VNA).

Figure 3: Shows the measured values of S_{21} of (a) substrate with 40% infill density & (b) substrate with 100% infill density.

2.1.1 Dielectric Constant

Calculating the dielectric constant requires a series of equations from (1) to (3), first, the effective dielectric constant by [7] is calculated from equation (1)

$$\epsilon_{r,eff} = \left(\frac{nc}{2\pi r_m f_o} \right)^2 \quad (1)$$

Where f_o is the nth resonant frequency of the ring, $\epsilon_{r,eff}$ is an effective ϵ_r , average radius of r_m , c speed of light in vacuum. After equation (1), equation (2) is used to calculate the dielectric constant of ABS:

$$\epsilon_r = \frac{2\epsilon_{r,eff} + M - 1}{M + 1} \quad (2)$$

where $M = \left(1 + \frac{12h}{W_{eff}} \right)^{-1/2}$, W_{eff} is the effective strip width for nonzero strip thickness,

$$W_{eff} = W + \left(\frac{1.25t}{\pi} \right) \left[1 + \ln \left(\frac{2h}{t} \right) \right] \quad (3)$$

W is width of the copper conductor, t is copper trace thickness, h is the thickness of ABS substrate. Using (1), (2), and (3), the calculation of values of dielectric constant at resonant peaks is done

2.1.2 Dielectric Loss

To calculate the dielectric loss ($\tan\delta$) following equation (4) is used:

$$\tan\delta = \frac{\alpha_d \lambda_o (\epsilon_r - 1) \sqrt{\epsilon_{r,eff}}}{8.686\pi \epsilon_r (\epsilon_{r,eff} - 1)} \quad (4)$$

where λ_o is wavelength of the resonant signal in the free space, α_d = dielectric attenuation factor. To calculate α_d following series of calculations are performed from equations (5) to (12).

Initially, in microstrip ring resonator the Q_o (unloaded) is obtained by [7], given in equation (5)

$$Q_o = \frac{Q_L}{1 - 10^{-\frac{L_A}{20}}} \quad (5)$$

where L_A is insertion loss of resonant peak in dB. The Q_L (loaded) is given in equation (6):

$$Q_L = \frac{f_o}{BW_{-3dB}} \quad (6)$$

where BW_{-3dB} is 3-dB bandwidth of the resonator. The total attenuation constant (α_{total}) is found using equation (7):

$$\alpha_{total} = \frac{\pi}{Q_o \lambda_g} \left[\frac{N_p}{\text{unit length } h} \right] \quad (7)$$

Where λ_g is the guided wavelength, sum of conductor factor (α_c), dielectric attenuation factor (α_d) and radiation attenuation factor (α_r), given in equation (8):

$$\alpha_{total} = \alpha_c + \alpha_d + \alpha_r \quad (8)$$

1) Conductor Attenuation Factor: Thickness of the strip is taken into account, conduction factor of a microstripping as in [8], given in equation (9):

$$\frac{W}{h} \leq \frac{1}{2\pi}$$

$$\alpha_c(f_o) = \frac{1}{2\pi} \frac{R_{s1}}{Z_o h} \left[1 - \left(\frac{W_{eff}}{4h} \right)^2 \right] \left\{ 1 + \frac{h}{W_{eff}} + \frac{h}{\pi W_{eff}} \left[\ln \left(\frac{4\pi W}{t} + 1 \right) - \frac{1 - \frac{t}{h}}{1 + \frac{t}{4\pi W}} \right] \right\} \left[\frac{N_p}{\text{unit length}} \right]$$

$$\frac{1}{2\pi} < \frac{W}{h} \leq 2$$

$$\alpha_c(f_o) = \frac{1}{2\pi} \frac{R_{s1}}{Z_o h} \left[1 - \left(\frac{W_{eff}}{4h} \right)^2 \right] \left\{ 1 + \frac{h}{W_{eff}} + \frac{h}{\pi W_{eff}} \left[\ln \left(\frac{2h}{t} + 1 \right) - \frac{1 - \frac{t}{h}}{1 + \frac{t}{4h}} \right] \right\} \left[\frac{N_p}{\text{unit length}} \right]$$

$$\frac{W}{h} > 2$$

$$\alpha_c(f_o) = \frac{R_{s1}}{Z_o h} \frac{1}{\left\{ \frac{W_{eff}}{h} + \frac{2}{\pi} \ln \left[2\pi e \left(\frac{W_{eff}}{2h} + 0.94 \right) \right] \right\}^2} \left[\frac{W_{eff}}{h} + \frac{\frac{W_{eff}}{\pi h}}{\frac{W_{eff}}{2h} + 0.94} \right] \left\{ 1 + \frac{h}{W_{eff}} + \frac{h}{\pi W_{eff}} \left[\ln \left(\frac{2h}{t} + 1 \right) - \frac{1 - \frac{t}{h}}{1 + \frac{t}{2h}} \right] \right\} \left[\frac{N_p}{\text{unit length } h} \right] \quad (9)$$

Where,

$$R_{s1} = R_s \left\{ 1 + \frac{2}{\pi} \tan^{-1} \left[1.4 \left(\frac{\Delta}{\delta_s} \right)^2 \right] \right\},$$

$$R_s = \sqrt{\frac{\pi \mu f_o}{\sigma}},$$

$$\delta_s = \sqrt{\frac{1}{\pi \mu \sigma f_o}}$$

R_{s1} is the surface-roughness resistance of the microstrip. R_s is the surface resistance of the microstrip. Z_o is the characteristics impedance of the microstrip. δ_s is the skin depth of copper. $\mu = 4 \pi \times 10^{-7}$ H/m, σ = bulk conductivity of the metal, f_o is the resonant frequency. Δ is the mean surface roughness of the copper trace.

- 2) Radiation Attenuation Factor: In this paper, radiation from the other parts of the structure is neglected while considering only radiation from the ring resonator. From Van der Pauw's work [9], the radiation quality factor Q_r of a ring resonator can be calculated using the given equation (10):

$$Q_r \approx \frac{4Z_o}{w^2 \mu^2 v_g^2 \left(1 - \frac{4}{3} \epsilon \mu + \frac{8}{15} \epsilon^2 \mu^2 \right)} \quad (10)$$

Where in this substrate, ϵ is permittivity and μ is permeability. Z_o is characteristic impedance. v_g is propagation velocity resonant signal. W is operating frequency. After restoring dimensions of dimensionless expression i.e., W , ϵ , μ , Z_o and v_g , following equation of Q_r is derived:

$$Q_r \approx \frac{\epsilon_r \text{eff } Z_o}{120 \pi^3 \left(\frac{h}{\lambda_o} \right)^2 \left(1 - \frac{4}{3} \epsilon_r + \frac{8}{15} \epsilon_r^2 \right)} \quad (11)$$

The radiation attenuation constant of the ring is given as equation (12)

$$\alpha_r = \frac{\pi}{Q_r \lambda_g} \left[\frac{N_p}{\text{unit length } h} \right] \quad (12)$$

where λ_g is the guided wavelength.

Finally, using equation (8) putting values of α_r , α_c , and α_{total} , the dielectric attenuation factor is obtained which is then used to determine loss tangent of ABS substrate using equation (4).

The calculated values of ϵ_r and $\tan \delta$ at 2.58 GHz and 2.59 GHz for substrates with 40% and 100% infill density respectively are shown in table 1, performing all the above calculations.

Table 1

Calculated values of the dielectric properties using the ring-resonator technique

Mode	Infill density	Resonant Frequency f_o	Insertion Loss $ S_{21} $	ϵ_r	$\tan \delta$
n = 1	40%	2.58 GHz	33.598 dB	2.62	0.0044
n = 1	100%	2.59 GHz	27.567 dB	2.59	0.0042

From Table 1, a difference of 0.03 can be observed in the dielectric constant. It was observed that the difference in dielectric constant is low due to more substrate thickness. A small dielectric loss difference of 0.0002 can be seen in Table 1

3. Conclusion

This paper talks about the characterization and comparison of results of 3D printed substrates for antenna design applications. The method of ring resonator is being used to calculate the dielectric properties of the substrate. For this analysis, a substrate of thickness 1mm was taken with the rectilinear infill pattern. Hence, it is observed that with the variation in substrate thickness, infill density, and infill pattern the dielectric properties of the substrate can be changed. The resulting values of dielectric constant and dielectric loss can be seen in Table 1. Figure 3 (a) & (b) shows the resonant frequency peaks for 40% infill density and 100% infill density respectively. This method is used on the highest and lowest viable infill densities to measure their dielectric properties and comparing them for the best one so that they can be used for microwave and RF applications.

4. References

- [1] O. A. Mohamed, *Analytical modeling and experimental investigation of product quality and mechanical properties in FDM additive manufacturing*. 2017.
- [2] A. Pizzagalli, T. Buisson, and R. Beica, "3D technology applications market trends & key challenges," in *ASMC (Advanced Semiconductor Manufacturing Conference) Proceedings*, 2014, pp. 78–81, doi: 10.1109/ASMC.2014.6846981.
- [3] B. T. Malik, V. Doychinov, S. A. R. Zaidi, I. D. Robertson, and N. Somjit, "Antenna Gain Enhancement by Using Low-Infill 3D-Printed Dielectric Lens Antennas," *IEEE Access*, vol. 7, pp. 102467–102476, 2019, doi: 10.1109/ACCESS.2019.2931772.
- [4] J. Huang, S. J. Chen, Z. Xue, W. Withayachumnankul, and C. Fumeaux, "Impact of Infill Pattern on 3D Printed Dielectric Resonator Antennas," in *Proceedings of the 2018 IEEE 7th Asia-Pacific Conference on Antennas and Propagation, APCAP 2018*, Nov. 2018, pp. 233–235, doi: 10.1109/APCAP.2018.8538296.
- [5] A. Rida, L. Yang, R. Vyas, and M. M. Tentzeris, *Conductive inkjet-printed antennas on flexible low-cost paper-based substrates for RFID and WSN applications*, vol. 51, no. 3. 2009, pp. 13–23.
- [6] L. Yang, A. Rida, R. Vyas, and M. M. Tentzeris, *RFID tag and RF structures on a paper substrate using inkjet-printing technology*, vol. 55, no. 12. 2007, pp. 2894–2901.
- [7] K. Chang, *Microwave Ring Circuits and Antenna*. New York, Wiley, 1994.
- [8] R. A. Pucel, D. J. Masse, and C. P. Hartwig, "Losses in microstrip," *IEEE Trans. Microwave Theory Tech.*, vol. MTT-16, pp. 342-350, June 1968.
- [9] L. J. van der Pauw, "The radiation of electromagnetic power by microstrip configurations," *IEEE Trans. Microwave Theory Tech.*, vol. MIT-25, pp. 719-725, June 1977.